Role of physical and chemical interactions in the antibacterial behavior of ZnO nanoparticles against E. coli

Jiang, Yunhong; Zhang, Lingling; Wen, Dongsheng; Ding, Yulong

DOI:
10.1016/j.msec.2016.08.044

Accepted Manuscript

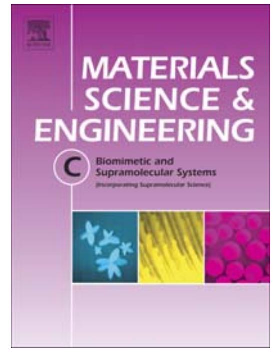

Role of physical and chemical interactions in the antibacterial behavior of ZnO nanoparticles against *E. coli*

Yunhong Jiang, Lingling Zhang, Dongsheng Wen, Yulong Ding

PII:	S0928-4931(16)30880-3
DOI:	doi: 10.1016/j.msec.2016.08.044
Reference:	MSC 6840

To appear in:	*Materials Science & Engineering C*

Received date:	9 May 2016
Revised date:	27 July 2016
Accepted date:	17 August 2016

Role of physical and chemical interactions in the antibacterial behavior of ZnO nanoparticles against *E. coli*

Yunhong Jiang[1], Lingling Zhang[2], Dongsheng Wen[1], Yulong Ding[3]*

1. Institute of Particle Science and Engineering, University of Leeds, Leeds, LS2 9JT, UK
2. School of Civil and Environmental Engineering, University of Science and Technology Beijing, China.
3. School of Chemical Engineering, University of Birmingham, B15 2TT, UK

Emails: y.jiang@leeds.ac.uk

ABSTRACT:

Zinc oxide (ZnO) nanoparticles (NPs) exhibit antibacterial activity against both Gram-positive and Gram-negative bacteria. However, the antimicrobial mechanism of ZnO NPs remains unclear. In this study, we investigated the interactions among ZnO NPs, released chemicals (Zn^{2+} and Reactive Oxygen Species, ROS) and *Escherichia coli* (*E. coli*) cells. ZnO NPs without contacting with bacterial cells showed strong antibacterial effect. The results of the leakage of intracellular K^+ and integrity of carboxyfluoresce in-filled liposomes showed that ZnO NPs have antimicrobial activity against *E. coli* by non-specifically disrupting *E. coli* membranes. Traces of zinc ions (1.25 mg/L) and hydrogen peroxide (from 1.25 to 4.5 μM/L) were detected in ZnO NPs suspensions, but was insufficient to cause the antibacterial effect. However, the addition of radical scavengers suppressed the bactericidal effect of ZnO coated films against *E. coli*, potentially implicating ROS generation, especially hydroxyl radicals, in the antibacterial ability of ZnO NPs.

Keywords:

ZnO NPs; Antibacterial Mechanism; Bio-interaction; *E. coli.*

1. INTRODUCTION

Zinc oxide (ZnO) nanoparticles (NPs) have received considerate attention recently due to their wide applications in a variety of areas, including chemistry, physics, materials science and the biomedical sciences. In particular, ZnO NPs have shown interesting antibacterial activities against both Gram-positive and Gram-negative bacteria such as spores. The majority of the studies are experimentally focused on a wide range of pathogenic and non-pathogenic microorganisms such as *Escherichia coli, Staphylococcus aureus and Bacillus subtilis* [1-16]. Several researchers have coated ZnO NPs on special substrates such as glass, paper and fibres for antimicrobial food packaging and antimicrobial healthcare materials [6-23].

However to date, the antibacterial mechanism of ZnO NPs has not been elucidated. Several possible mechanisms have been postulated on the bactericidal effect of ZnO NPs from both physical and chemical interaction aspects. Zinc ions and radical oxygen species (ROS) are main chemicals released from ZnO coated film. Yamamoto et al. [23] studied the antibacterial behavior of ZnO NPs using chemiluminescence and oxygen electrode analysis. They reported that H_2O_2 generated from ZnO penetrated the cell membrane of *E. coli*, and inhibited the growth of the cells. H_2O_2 concentrations ranging from 0.13 to 0.95 mol/L were detected in ZnO powder suspension [24]. However, Yang et. al. and Tam et. al. reported that the release of Zn^{2+} ions as a result of ZnO decomposition may instead be responsible for the observed antibacterial activity [11, 26]. In addition, the electrostatic interaction between ZnO NPs and bacteria cell surface may play an important role [2]. SEM analysis of the morphological changes of *E. coli* exposed to ZnO NPs has been conducted by Zhang et al. [7]. They suggested that the interaction of ZnO NPs and cell membrane could underlie the antibacterial effect, since treatment with ZnO NPs appeared to prompt the damage and subsequent breakdown of *E. coli* membranes.

Such a short review shows that the dominant mechanisms responsible for antibacterial activity of ZnO NPs still remain to be established. Most of the published studies were focused on ZnO dispersions, and few on ZnO-coated films, whose comparison was even rare. It shall be also noted that many commercial ZnO nanoparticles were used, and the morphology of ZnO in the liquid phase was highly dependent on the surfactants or dispersants used, which themselves would introduce some side-effects. A proper characterization of ZnO dispersions is of high value to elucidate the mechanisms. The fully physical and chemical characterizations of nanoparticles can help reviewer to have a better understanding and give a good repeatability for the experiment. This work aimed to conduct a detailed anti-bacteria experiment using well-characterized ZnO NPs and to reveal the underneath mechanisms. The ZnO particle size, shape, film porosity, colloidal stability and surface charge were carefully characterized to avoid unpredictable outcomes. Although ZnO NPs showed a strong antibacterial activity on both Gram-positive and Gram-negative bacteria, Gram-negative bacteria *E. coli* was selected for investigating the interactions between ZnO NPs and bacteria cell due to they are large, easy to observe and well-understood organisms. The physical and chemical interactions between ZnO NPs and *E.coli* cells were investigated.

2. MATERIALS AND METHODS

2.1. Preparation of ZnO NPs and ZnO coated films.

Dry ZnO NPs (sized 90~200 nm) were purchased commercially from Nanostructured & Amorphous Materials (USA) in this work. A stock suspension was prepared by resuspending the NPs in MilliQ water to produce a final concentration of 20 g/L. The pH of the suspension was adjusted to be the same as the culture medium, i.e. ~7.2, by using NaOH (1 M, Fisher Scientific, UK) and HCl (0.1 M, Fisher Scientific, UK). To prepare the coated film, a master suspension with a concentration of 5.0 g/L was prepared by mechanical milling in a Dyno-Mill (Willy A. Bachofen, Switzerland) with Zircon based beads (diameter 0.2 μm). The blank films were cleaned by ultrasonication for 5 min. The master suspension was coated uniformly using glass coater onto one side of the PVC film. After drying at room temperature, the coated PVC films were spread on a poly methyl methacrylate plastic substrate, and were subsequentlyroasted and pressed at 100 ℃ for 10 min. Morphology was characterized by scanning electron microscopy (SEM) and transmission electron microscopy (TEM). SEM analyses was conducted on a LEO Gemini 1530 field emission SEM operating at a voltage of 5kV [7], and TEM on a Philips FEI Tecnai TF20 field emission gun TEM operating at a gun voltage of 200 kV, fitted with an Oxford Instruments INCA 350 EDX system/80 mm X-Max silicon drift detector and Gatan Orius SC600A charge-coupled device camera. Characterisation by XRD was carried out using a PANalytical X´Pert diffractometer operating with a Cu Kα radiation source (λ=1.541Å). Zeta potentials of all the samples were determined in order to obtain information on the surface charge of ZnO NPs, measured by a Zetasizer (Malvern Instruments, UK) at 25 ℃. The experiments were performed using 50 ml polyethylene tubes and the concentrations of ZnO solutions were 2, 1, 0.5, 0.2, 0.1 g/L. The pH value of ZnO suspension was around 7.2. The samples were shaken by a bath shaker with a 200 rpm speed under room temperature for 48 hour.

For separation, the samples were centrifuged at 11000×g for 5 min. The clear supernatant samples were filtered by a 0.1 μm Filter (Whatman), and then the concentration of zinc ions in the solution were measured by a Varian model Spectra atomic absorption spectrometer (Australia). The operating conditions were as follows: wavelength, 213 nm; lamp current, 5.0 mA; acetylene flow, 1.5 L/min. Standard solutions of 0.5 ppm, 1.0 ppm, 1.5 ppm and 2.0 ppm were used to calibrate the system prior to use and three measurements were taken from each aliquot in order to determine the mean concentration of zinc at each time interval.

2.2. Evaluating antibacterial activity.

Culture turbidity was measured at 600nm to assess the bacterial cell growth, and the cultures were plated onto agar to determine viable counts. To prevent a photocatalytic effect with ZnO NPs, all experiments were performed in the dark. *Escherichia coli* strain DH5α (obtained from the Faculty of Biological Sciences, University of Leeds, UK) was cultured in Luria-Bertani (LB) broth medium (Sigma-Aldrich, UK) with a 200 rpm shaking under aerobic conditions at 37 ℃ for 18 h. The culture was diluted to give approximately 1×10^{6}-10^{7} colony forming units/ml (CFU). Three replicate tubes were prepared for each treatment. In a typical experiment, 50 μl of the diluted culture of *E. coli* was inoculated into 20 ml LB broth containing ZnO coated films. The mixture was cultured under aerobic conditions at 37 ℃. Viable cell numbers were followed by plating diluted cultures onto LB agar, incubating the plates for 48 h at 37 ℃, and then enumerating colonies. In order to determine the antibacterial activity of zinc ions, $ZnCl_2$ was employed to culture with *E. coli* in LB broth under conditions described above and NaCl was used to eliminate the effect of Cl^-.

2.3. Antibacterial mechanisms of ZnO NPs.

In order to prevent the potential penetration and physical contact between ZnO NPs and bacterial cells, ZnO NPs were firmly coated on the PVC films. A set of tests were performed using a membrane barrier which physically separated the ZnO coated films from the bacteria during the antibacterial tests. This membrane, whilst preventing direct physical contact, would nonetheless allow diffusible factors (including ions or ROS, but not bacteria or NPs) produced by ZnO NPs to pass through and mediate the antibacterial effect. A Vivascience Vivaspin tube (Ultra 100,000MWCO), with a true pore size <50 nm, was used. LB broth (10 ml) was added into the left part of the tube with the ZnO coated film, while the right-hand side of the tube contained 10 ml LB and *E. coli* (10^{6-7} CFU). Aliquots (100 μL) of *E. coli* culture (10^{6-7} CFU) were transferred to the right side of the tube and cultured under aerobic conditions at 37 ℃. Blank PVC films were used to provide a negative control. Viable cell numbers were followed by plating diluted cultures onto LB agar, and incubating the plates for 48 h at 37 ℃, before counting colonies. Hydrogen peroxide produced by ZnO NPs was measured by Amplex Red Hydrogen Peroxide ATP Determination Assay Kit (Molecular Probes, UK). The working solution of 100 μM Amplex Red reagent and 0.2 U/mL horseradish peroxidise (HRP) were prepared by using the reaction buffer. A series of concentrations, i.e., 10 μM, 5 μM, 2.5 μM, 1.25 μM, 0.625 μM, 0.3125 μM of H_2O_2, was prepared using the reaction buffer. The ZnO suspensions with different concentrations were prepared. At designated points, 50 μL of the standard solutions, ZnO suspensions, and reaction buffers were transferred to 96-well microplates. Amplex UltraRed fluorescence then was measured with an excitation at 544nm and fluorescence emission at 590nm in Fluo star optima (BMG labtech Ltd., UK). Each sample was tested 3 times to obtain statistically meaningful results. The reaction buffer was used as the negative control and to help correct the background of fluorescence measurements. The free radical scavengers including vitamin E, mannitol and gluthathione were employed to quench the release of ROS produced by ZnO NPs and block the antibacterial effect of the coated films.

2.4. Evaluating membrane damage.

The effect of the ZnO NPs on the membrane integrity of *E. coli* DH5α cells through the leakage of K^+ monitored was assessed by atomic absorption spectroscopy. Cells were resuspended in 5mM HEPES 5mM Glucose buffer (pH 7.2), as described previously[30] To examine the action of ZnO NPs over a time course against *E. coli* DH5α cells, we assessed the ability of the ZnO NPs to compromise the integrity of carboxyfluorescein-filled liposomes made of a phospholipid content of *E. coli* CM (approximately 70% [wt/wt] phosphatidylethanolamine, 20% phosphatidylglycerol, 10% cardiolipin) [27, 28]. Phospholipids were from Avanti polar lipids (Birmingham, AL). The leakage of carboxyfluorescein from the liposomes was monitored at 485nm and the percent of liposome integrity was calculated relative to liposomes challenged with 0.5% Triton X-100 (corresponding to 100% liposome damage [0% liposome integrity]) [28]. In both methods antibiotic agents were at 4 x MIC using 5 % SDS an appropriate control for membrane damage, and over a 180 minute time course, taking readings at 0, 10, 60 and 180 minutes. Each method was carried out for at least three biological replicates.

3. RESULTS AND DISCUSSION

3.1. Characterizations of ZnO NPs and ZnO coated films.

The effects of milling on the physical properties of the ZnO powder were assessed by Transmission Electron Microscopy (TEM) and showed in Figure 1. The results showed that the ZnO NPs were generally presenting as clusters and some were in the micronmeter size range before milling (Figure 1a). The size distribution decreased with increasing milling time. After milling, the particle sizes were more homogeneous, ranging from 20 to 50 nm, with an average particle size of around 30 nm. The inset in Figure 1b is of the cluster of particles visible in Figure 1b. The high resolution TEM image in Figure 1b showed highly crystalline materials.

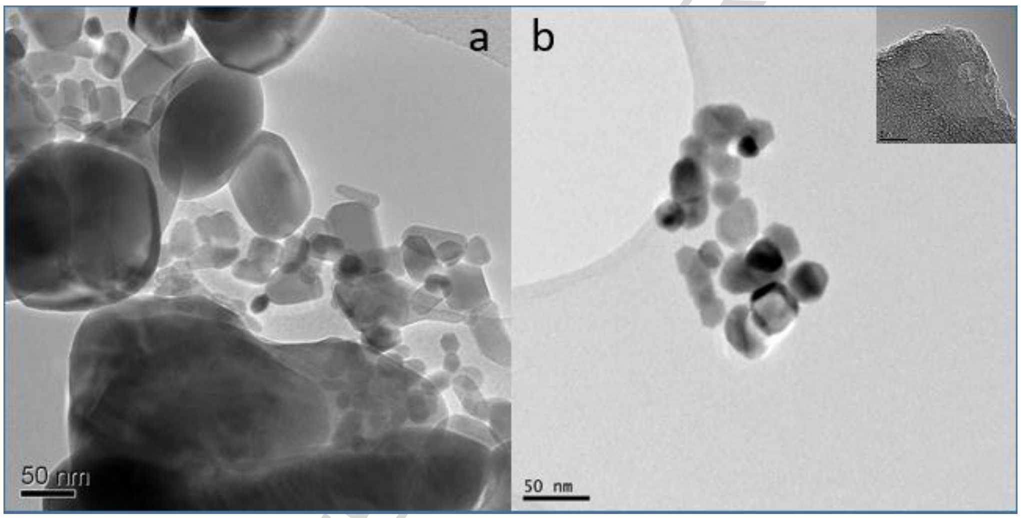

Figure 1. TEM micrograph of the ZnO NPs: Before milling (a) a typical cluster of particles with varying morphologies present in the sample; After milling (b) a typicla cluster of particles with similar morphologies present in the sample.

Particle size distribution data obtained by DLS for NPs suspended in water at a final solution pH of 7.2 were shown in (SI Appendix Fig. 1). There was a little difference with the TEM primary particles size (20-50 nm) compared to the results of Zetasizer (ranging from 20 nm to 80 nm) due to the presence of agglomerates. The surface morphology of ZnO NPs was observed by SEM and shown in (SI Appendix Fig. 2). The crystallite and primary particle sizes here were consistent with TEM results. Figure 2 showed the XRD patterns for the ZnO NPs after milling with the Miller indices of the planes indicated above each peak. The peaks in the pattern were consistent with that of the JCPDS reference file for the hexagonal-close-packed wurtzite structure of zincite (ref: 01-079-0206). The XRD results indicated clearly that the main crystalline phase was hexagonal zincite structure. No diffraction lines associated with impurities were detected. The average crystallite size was estimated from the peaks using the Debye-Scherer formula. By applying Scherrer equation (1) on the XRD pattern, the particle size can be calculated:

$$D = K\lambda / (\beta \cos\theta) \quad (1)$$

Where D is the mean size of crystallites (nm), K is Scherrer constant. K = 0.89 if β is the full width at half the maximum in radians of the X-ray diffraction peak; K = 1 if β is integral height to width of the diffraction peak. Θ is diffraction angle (deg) [29]. The average crystallite size of ZnO NPs was 43 ± 8 nm.

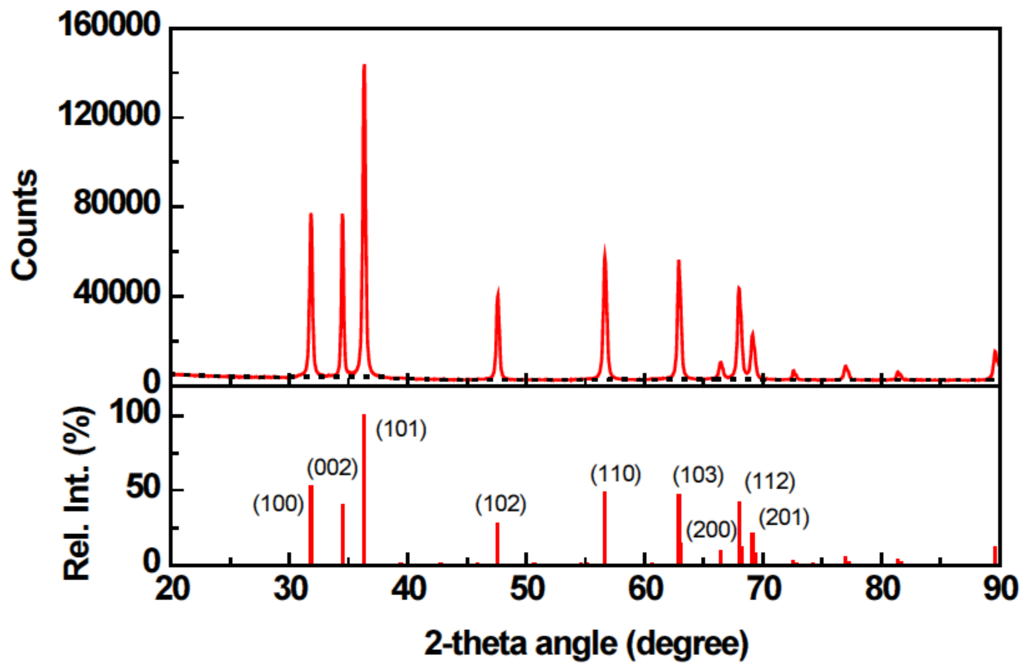

Figure 2. The results of X-ray diffraction for the ZnO NPs after the milling. Phase analysis of ZnO NPs was achieved by XRD using a Philips PANaltical X'Pert X-Ray diffractometer with a Cu Kα X-ray scource scanning over a range of 20-90^{o} 2θ.

The zeta-potential of ZnO suspension was approximately +40 mV at pH value of 7.2. There is no significant difference before and after milling in terms of the surface charge (SI Appendix). The coated films were prepared as described above. The ZnO NPs were found to be firmly coated on the surface of films. There were no big cracking sign on the surface of zinc oxide coated films, namely the NPs were evenly distributed on the surface. The sizes of particles embedded on the surface ranged from 30 nm to 80 nm due to the presence of aggregation (SI Appendix Fig. 3). The ZnO NPs were coated on the surface of the films uniformly, and the size of and shape of ZnO NPs on the surface of PVC films had not changed upon coating. The amounts of ZnO NPs film disc ranged from 100 to 50 μg/cm^2. The BET value of ZnO coated films ranged from 26.38 m^2/g to 33.07 m^2/g depending on the concentration of ZnO NPs on the surface of films. The further thermal stability and morphology of ZnO coated films is described in a previous paper [8].

3.2. Antibacterial activity of ZnO NPs without physical interaction

The membrane barrier with 50 nm pore size was employed to separate the organisms from the ZnO coated films. Figure 3 showed that whilst ZnO coated films with the membrane barrier retained some degree of antibacterial activity, the antibacterial effect was diminished compared to experiments run in the absence of the membrane barrier. Because ZnO NPs have been firmly coated on the surface of films and totally separated by membrane barrier, there was no physical interaction between ZnO NPs and bacterial cells. These results suggested that the antibacterial activity of ZnO coated films was blocked at least in part by the membrane barrier. It indicated physical interactions between ZnO NPs and cell had partial contribution to the antibacterial behavior of ZnO NPs. Furthermore, the results implied that due to the killing by diffusible factors, some chemicals released by ZnO coated films passed through the membrane barrier and killed the bacteria.

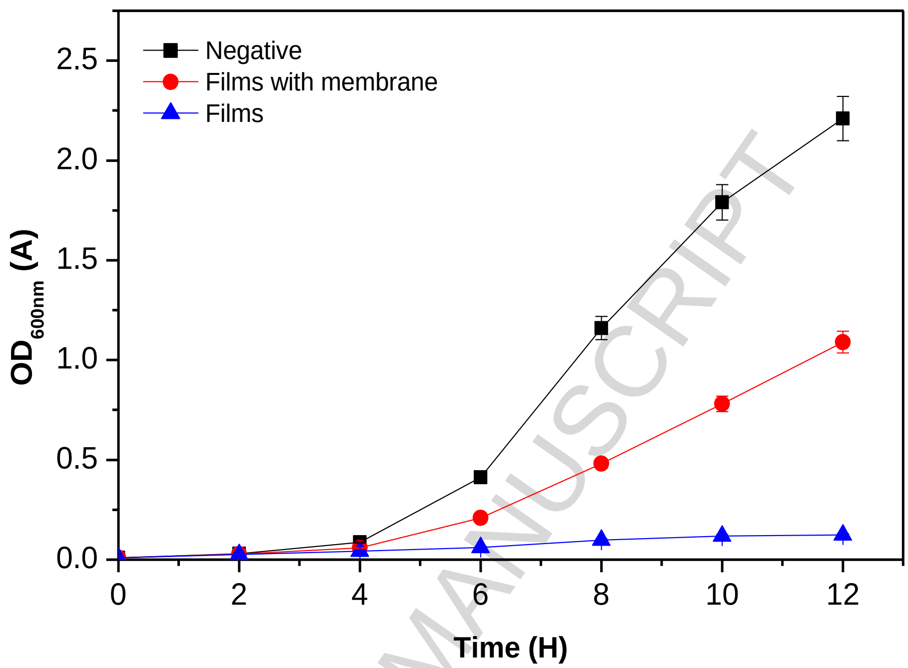

Figure 3. Growth curves of *E. coli* in LB medium inoculated with 10^7 CFU of bacteria in the presence of ZnO coated films with and without membrane barrier. Growth analysis curves measured by monitoring the optical density (OD) at 600 nm.

3.3. Membrane damage:

To confirm that ZnO NPs caused cell death through membrane damage, we performed an assay which assessed this property further by quantifying the leakage of the intracellular component K^+ from whole *E. coli* DH5α cells resuspended in 5mM HEPES 5mM Glucose (pH7.2) buffer. This allowed us to evaluate the *E. coli* bacterial membrane integrity, not just the cytoplasmic membrane (Figure 4). After 60 minutes with ZnO NPs, the percentage of K^+ remaining was zero, suggesting a complete loss of membrane integrity. For the negative control Tetracycline, 100% K^+ was remained after 180 minutes, indicating no membrane damage. It is of note that 5% SDS also had an extensive effect on the loss K^+ from the cells over 180 minutes but the loss was much slower than ZnO NPs.

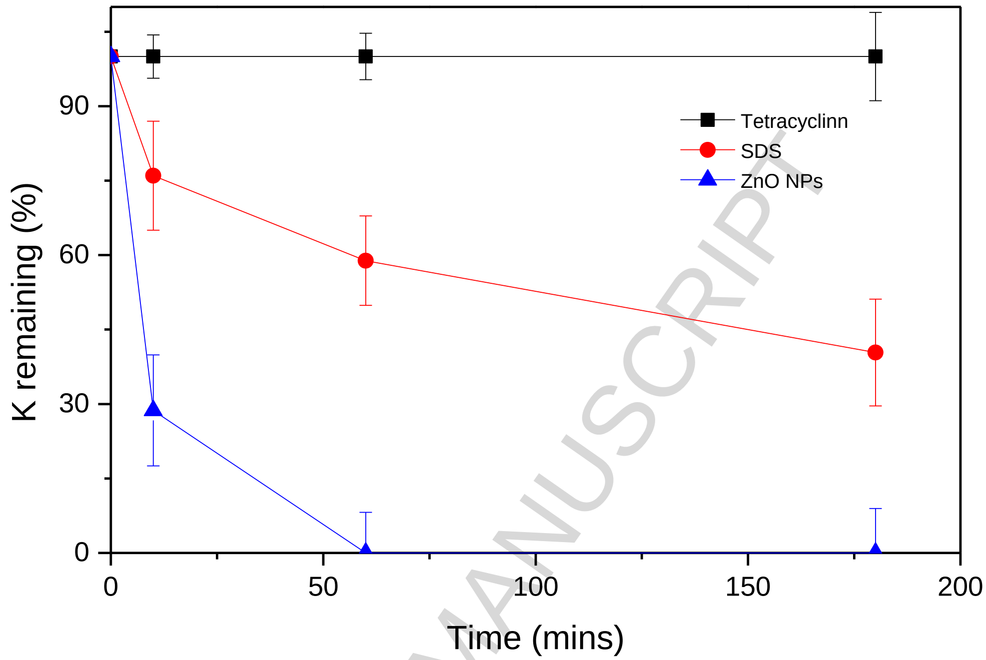

Figure 4. The effect of ZnO NPs and comparator agents on the retention of K^+ by *E. coli* DH5α over a 180 minute time course. At time zero Tetracycline and ZnO NPs were added at 4 x MIC, and SDS at 5%. Aliquots were taken at times described in the methods.

Such evidence indicates clearly that ZnO NPs' antimicrobial activity against *E. coli* was through non-specifically disrupting the *E. coli* membranes. As mentioned previously the leakage of carboxyfluorescein from liposomes was monitored at 485 nm, and the percentage of liposome integrity was calculated relative to liposomes challenged with 0.5% Triton X-100 (corresponding to 100% liposome damage [0% liposome integrity]) [28]. Over a 180 minute time course, ZnO NPs led to >65% loss of integrity, compared to the negative control Tetracycline, which maintained 100% integrity. Whilst as expected, the positive control 5% SDS had full loss of integrity after 60 minutes (Figure 5). These findings suggested that ZnO NPs caused cell death by directly interacting with the phospholipid bilayer of the membrane, causing loss of membrane integrity, as shown by the leakage of trapped carboxyfluorescein dye.

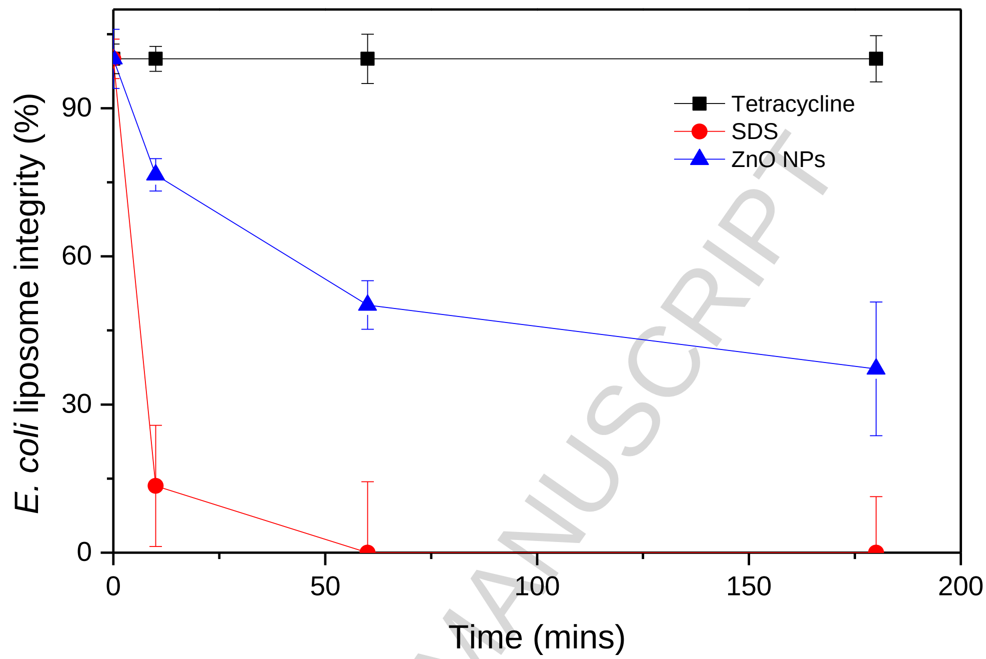

Figure 5. The effect of ZnO NPs and comparator agents on the integrity of carboxyfluorescein filled liposomes over a 180 minute time course. At time zero Tetracycline and ZnO NPs were added at 4 x MIC, and SDS at 5%. Aliquots were taken at times described in the methods.

Several possible mechanisms were proposed to explain the attachment of ZnO NPs to the bacterial surface: Van der Waals forces, electrostatic, hydrophobic and receptor-ligand interactions [30, 31]. In this work, ZnO NPs were positively charged (+40 mV) on the surface at pH 7.2. In contrast, the bacterial cell envelope had an overall negative charge (-33.9 mV) due to the presence of lipopolysaccharides [32]. It would be plausible that the electrostatic attraction between negatively charged bacterial cells and positively charged ZnO NPs were responsible for the attachment. It can be concluded that the antimicrobial ability of the ZnO NPs was closely related to the disruption of the membrane integrity through the direct contact with bacterial cell. The intrinsic toxic properties of ZnO played an important role, causing structural changes and degradation of cell.

3.4. Possible antibacterial mechanism of Zn^{2+} released from dissolution of ZnO NPs.

One of an early study suggested that the antibacterial activity of ZnO NPs could result from dissolved metal ions from oxide [1]. To check on this point, we firstly determined the antibacterial behavior of zinc ions. Cell experiments using $ZnCl_2$ as a source of zinc ions were performed, which showed that there was no cell death observed for the zinc ion concentration up to 10 mg/L (SI Appendix Fig. 4). Secondly, the amount of Zn^{2+} released from ZnO NPs was measured by an atomic absorption spectroscopy (AAS). Figure 6 showed that the concentration of Zn^{2+} released from ZnO NPs at concentration of 0.2 g/L was around 1.25 mg/L. Even the concentration of ZnO NPs was increased to 2 g/L, the concentration of released zinc ions would be still much smaller than the needed 100 mg/L to produce any cell death. However consistent with previous result [7], we have shown that the MIC of ZnO NPs against *E. coli* was 0.2 g/L. Clearly the chemical interactions between zinc ions and bacterial cell are unlikely to be a plausible antibacterial mechanism of ZnO NPs against *E. coli*.

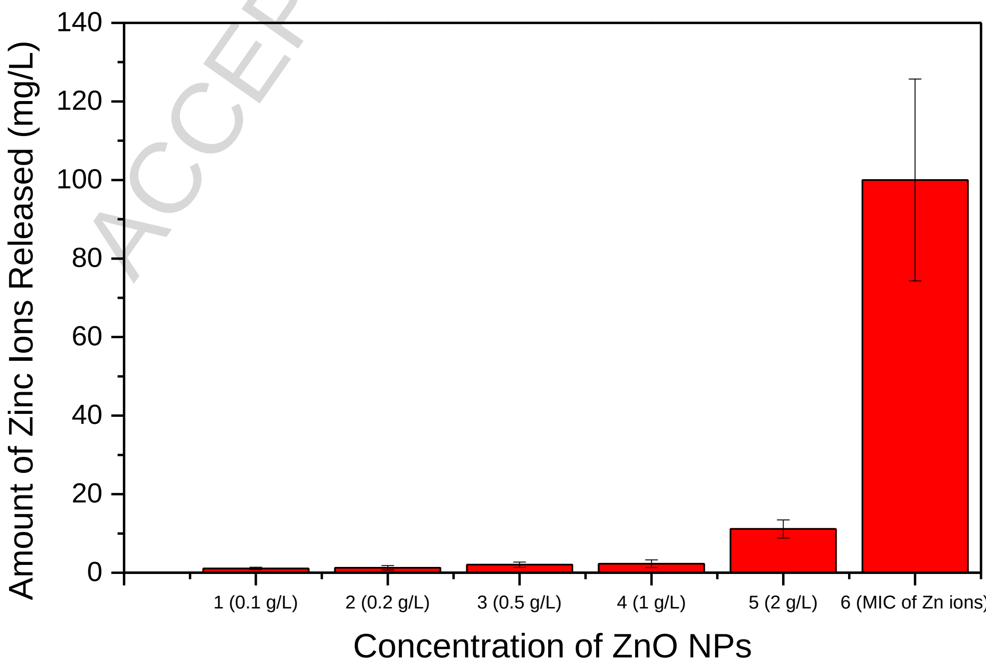

Figure 6. Amount of Zinc ions released from ZnO NPs as a function of concentrations. The concentrations of the ZnO solutions were 2, 1, 0.5, 0.2, 0.1 g/L at pH 7.2.

3.5. Possible antibacterial mechanism of the generation of reactive oxygen species (ROS).

The generation of ROS has been known to contribute to ZnO NPs antibacterial activity [31]. In this study, radical scavengers (Mannitol, Vitamin E and Glutathione (GSH)) were employed to indirectly assess whether radical formation was responsible, because they can alter the kinetic profile of the reaction. Figure 7 showed that the addition of radical scavengers suppressed the level of the bactericidal effect of ZnO coated films against *E. coli*. The survival number of *E. coli* with scavengers in the absence of ZnO coated films was almost the same as the negative control, indicating that scavengers themselves had no effect on cell viability. The results also showed that the antibacterial ability of ZnO NPs was inhibited by the quenching agents.

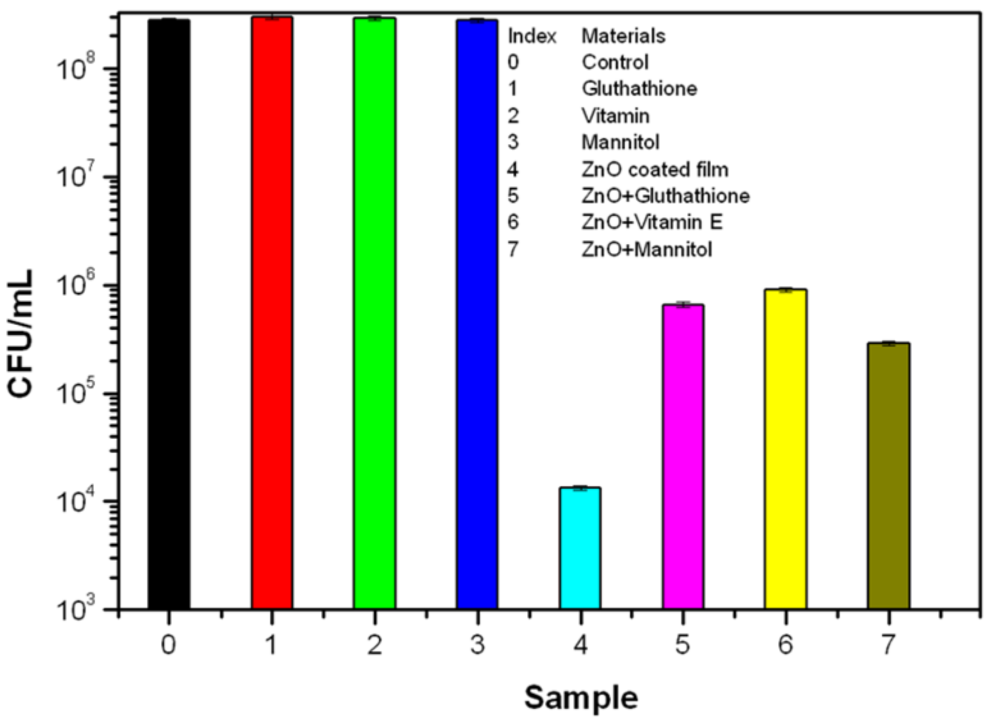

Figure 7. The ROS contribute to the lethality elicited by ZnO NPs. Growth curves of *E. coli* in LB medium inoculated with 10^7 CFU of bacteria in the presence of ZnO coated films with 100 mM quenching agents (including vitamin E, mannitol, gluthathione).

In this assay, the amounts of hydrogen peroxide in ZnO solution were measured by Amplex Red Hydrogen Peroxide Assay Kit. For ZnO NPs with average size of 1000 nm, the concentration of H_2O_2 was observed to increase from 1.25 to 4.5 µM/L as ZnO concentration was increased from 0.1 g/L to 0.4 g/L (Figure 8). In addition, the hydrogen peroxide was not observed in ZnO NPs suspension with average size of 100nm. However, separated experiments on the susceptibility determinations with hydrogen peroxide against *E. coli* showed that the MIC value was 0.5 mM/L (SI Appendix Fig. 5), which is two orders of magnitude higher than those released from ZnO. Clearly ZnO NPs did not produce sufficient amount of hydrogen peroxide even at high concentrations of ZnO NPs to have produce any bactericidal effect.

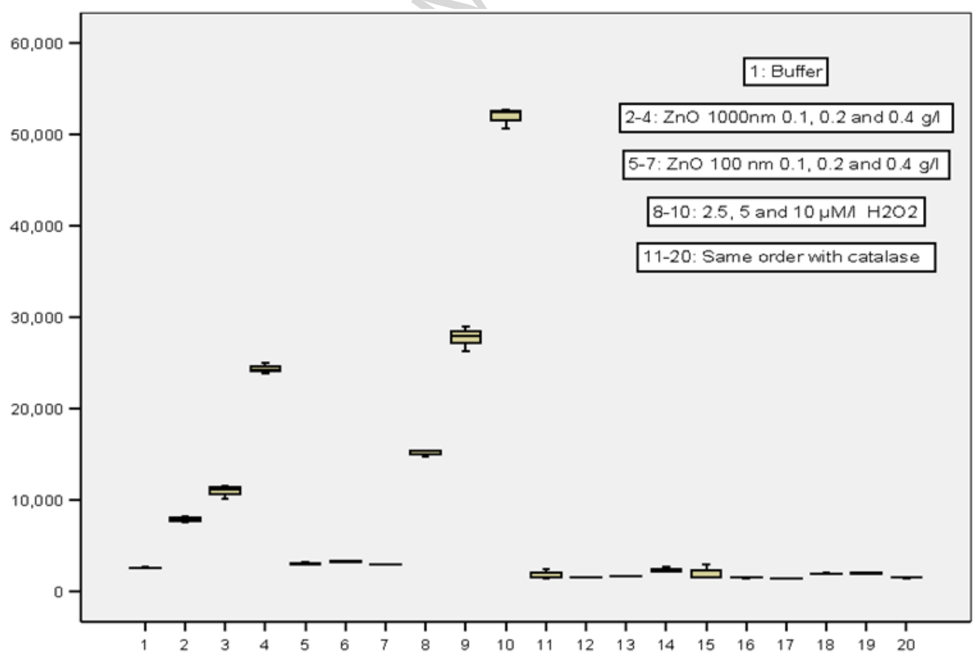

Figure 8. The amount of hydrogen oxide in the presence of ZnO particles with catalase – the hydrogen oxide measurement is made using Amplex Red.

There are other potential ROS that could be produced by ZnO NPs such as hydroxyl radical and superoxide anion. Superoxide anion radical is unlikely to cause any bactericidal effect as it is less toxic and is poorly permeating to cell membranes [18, 34-37]. However hydroxyl radical is the most reactive oxygen radical known. It would react very quickly with almost every type of molecule found in living cells. The reactivity of hydroxyl radical is so great that, if they are formed in living systems, they will react immediately with whatever biological molecule is in their vicinity, producing secondary radicals of variable reactivity [1, 10, 18, 34-36, 38-43]. Applerot et al showed that aqueous suspensions of ZnO with small particle size produce higher level of hydroxyl radicals by using electron-spin resonance measurement. Hydroxyl radicals were present in water supensions of ZnO, their number being closely related to the size of the ZnO particles, with smaller sizes having a greater number of ·OH. In addition, the ROS level increased up to nearly 400% with visible light emitted from a lamp compared to susupensions without illumination [12, 18]. The same finding has been reported by Palominos et al [44]. Therefore, it may be suggested that regarding the ROX effect, hydrogen peroxide and superoxide anion production from ZnO NPs would not produce salient antibacterial effect. Instead, the hydroxyl radicals may contribute to the antibacterial properties of ZnO NPs.

4. CONCLUSION

This work reported the potential antibacterial mechanisms of ZnO NPs against *E. coli* cells. The antibacterial results of ZnO NPs without contacting bacterial cells showed that both physical and chemical interactions contributed to the antibacterial behavior of ZnO NPs. The results of the leakage of intracellular K^+ and integrity of carboxyfluoresce in-filled liposomes showed that ZnO NPs caused cell death by directly interacting with the phospholipid bilayer of the membrane, causing loss of membrane integrity. Furthermore, the addition of radical scavengers suppressed the bactericidal effect of ZnO coated films against *E. coli*, potentially implicating the ROS generation in ZnO NPs played an important role in the antibacterial properties of ZnO NPs. Certain concentrations of zinc ions and hydrogen peroxide were detected in ZnO NP suspensions. However, the concentration of zinc ions and hydrogen peroxide were insufficient to cause any antibacterial effect. The hydroxyl radical may contribute to the antibacterial properties of ZnO NPs. However, there are a number of questions remained to be answered before a firm conclusion could be drawn. Further study is needed to identify the contribution of hydroxyl radicals on the chemical interaction of ZnO NPs against E.coli bacteria.

ACKNOWLEDGMENTS

We would like to thank Dr. Alex O'Neill and Miss Anna Lippell of Leeds University Faculty of Biological Science for help with the biology tests and support in the interpretation of the presented results.

REFERENCES

[1] J. Sawai, S. Shoji, H. Igarashi, A. Hashimoto, T. Kokugan, M. Shimizu and H. Kojima, Hydrogen peroxide as an antibacterial factor in zinc oxide powder slurry, Journal of Fermentation and Bioengineering, 86 (1998) 521-522.

[2] P.K. Stoimenov, R.L. Klinger, G.L. Marchin and K.J. Klabunde, Metal oxide nanoparticles as bactericidal agents, Langmuir, 18 (2002) 6679-6686.

[3] J. Sawai, Quantitative evaluation of antibacterial activities of metallic oxide powders (ZnO, MgO and CaO) by conductimetric assay, Journal of Microbiological Methods, 54 (2003) 177-182.

[4] L.K. Adams, D.Y. Lyon and P.J.J. Alvarez, Comparative eco-toxicity of nanoscale TiO2, SiO2, and ZnO water suspensions, Water Research, 40 (2006) 3527-3532.

[5] R. Brayner, R. Ferrari-Iliou, N. Brivois, S. Djediat, M.F. Benedetti and F. Fievet, Toxicological impact studies based on Escherichia coli bacteria in ultrafine ZnO nanoparticles colloidal medium, Nano Letters, 6 (2006) 866-870.

[6] N.M. Franklin, N.J. Rogers, S.C. Apte, G.E. Batley, G.E. Gadd and P.S. Casey, Comparative toxicity of nanoparticulate ZnO, bulk ZnO, and ZnCl2 to a freshwater microalga (Pseudokirchneriella subcapitata): The importance of particle solubility, Environmental Science & Technology, 41 (2007) 8484-8490.

[7] L.L. Zhang, Y.H. Jiang, Y.L. Ding, M. Povey and D. York, Investigation into the antibacterial behaviour of suspensions of ZnO nanoparticles (ZnO nanofluids), Journal of Nanoparticle Research, 9 (2007) 479-489.

[8] Y.H. Jiang, A.J. O'Neill and Y.L. Ding, Zinc oxide nanoparticle-coated films: fabrication, characterization and antibacterial properties, Journal of Nanoparticle Research, 17 (2015) 2993-2996.

[9] Z.B. Huang, X. Zheng, D.H. Yan, G.F. Yin, X.M. Liao, Y.Q. Kang, Y.D. Yao, D. Huang and B.Q. Hao, Toxicological effect of ZnO nanoparticles based on bacteria, Langmuir, 24 (2008) 4140-4144.

[10] N. Jones, B. Ray, K.T. Ranjit and A.C. Manna, Antibacterial activity of ZnO nanoparticle suspensions on a broad spectrum of microorganisms, Fems Microbiology Letters, 279 (2008) 71-76.

[11] K.H. Tam, A.B. Djurisic, C.M.N. Chan, Y.Y. Xi, C.W. Tse, Y.H. Leung, W.K. Chan, F.C.C. Leung and D.W.T. Au, Antibacterial activity of ZnO nanorods prepared by a hydrothermal method, Thin Solid Films, 516 (2008) 6167-6174.

[12] G. Applerot, A. Lipovsky, R. Dror, N. Perkas, Y. Nitzan, R. Lubart and A. Gedanken, Enhanced Antibacterial Activity of Nanocrystalline ZnO Due to Increased ROS-Mediated Cell Injury, Advanced Functional Materials, 19 (2009) 842-852.

[13] Y. Liu, L. He, A. Mustapha, H. Li, Z.Q. Hu and M. Lin, Antibacterial activities of zinc oxide nanoparticles against Escherichia coli O157:H7, Journal of Applied Microbiology, 107 (2009) 1193-1201.

[14] B. Wu, Y. Wang, Y.H. Lee, A. Horst, Z.P. Wang, D.R. Chen, R. Sureshkumar and Y.J.J. Tang, Comparative Eco-Toxicities of Nano-ZnO Particles under Aquatic and Aerosol Exposure Modes, Environmental Science & Technology, 44 (2010) 1484-1489.

[15] K.M. Reddy, K. Feris, J. Bell, D.G. Wingett, C. Hanley and A. Punnoose, Selective toxicity of zinc oxide nanoparticles to prokaryotic and eukaryotic systems, Appl Phys Lett, 90 (2007) 2139021-2139023.

[16] L. Zhang, Y. Jiang, Y. Ding, N. Daskalakis, L. Jeuken, M. Povey, A. O'Neill and D. York, Mechanistic investigation into antibacterial behaviour of suspensions of ZnO nanoparticles against E. coli, Journal of Nanoparticle Research, 12 (2010) 1625-1636.

[17] K. Ghule, A.V. Ghule, B.J. Chen and Y.C. Ling, Preparation and characterization of ZnO nanoparticles coated paper and its antibacterial activity study, Green Chemistry, 8 (2006) 1034-1041.

[18] G. Applerot, N. Perkas, G. Amirian, O. Girshevitz and A. Gedanken, Coating of glass with ZnO via ultrasonic irradiation and a study of its antibacterial properties, Applied Surface Science, 256 (2009) S3-S8.

[19] S.D. Gittard, J.R. Perfect, N.A. Monteiro-Riviere, W. Wei, C.M. Jin and R.J. Narayan, Assessing the antimicrobial activity of zinc oxide thin films using disk diffusion and biofilm reactor, Applied Surface Science, 255 (2009) 5806-5811.

[20] J.H. Ji and W. Zhang, Bacterial behaviors on polymer surfaces with organic and inorganic antimicrobial compounds, Journal of Biomedical Materials Research Part A, 88A (2009) 448-453.

[21] J.H. Li, R.Y. Hong, M.Y. Li, H.Z. Li, Y. Zheng and J. Ding, Effects of ZnO nanoparticles on the mechanical and antibacterial properties of polyurethane coatings, Progress in Organic Coatings, 64 (2009) 504-509.

[22] I. Perelshtein, G. Applerot, N. Perkas, E. Wehrschetz-Sigl, A. Hasmann, G.M. Guebitz and A. Gedanken, Antibacterial Properties of an In Situ Generated and Simultaneously Deposited Nanocrystalline ZnO on Fabrics, Acs Applied Materials & Interfaces, 1 (2009) 363-366.

[23] G. Applerot, R. Abu-Mukh, A. Irzh, J. Charmet, H. Keppner, E. Laux, G. Guibert and A. Gedanken, Decorating Parylene-Coated Glass with ZnO Nanoparticles for Antibacterial Applications: A Comparative Study of Sonochemical, Microwave, and Microwave-Plasma Coating Routes, Acs Applied Materials & Interfaces, 2 (2010) 1052-1059.

[24] O. Yamamoto, M. Komatsu, J. Sawa and Z.E. Nakagawa, Effect of lattice constant of zinc oxide on antibacterial characteristics, Journal of Materials Science-Materials in Medicine, 15 (2004) 847-851.

[25] T. Xu and C.S. Xie, Tetrapod-like nano-particle ZnO/acrylic resin composite and its multi-function property, Progress in Organic Coatings, 46 (2003) 297-301.

[26] Z.H. Yang and C.S. Xie, Zn^{2+} release from zinc and zinc oxide particles in simulated uterine solution, Colloids and Surfaces B-Biointerfaces, 47 (2006) 140-145.

[27] C. StGelais, T.J. Tuthill, D.S. Clarke, D.J. Rowlands, M. Harris and S. Griffin, Inhibition of hepatitis C virus p7 membrane channels in a liposome-based assay system, Antiviral research, 76 (2007) 48-58.

[28] C.P. Randall, K.R. Mariner, I. Chopra and A.J. O'Neill, The target of daptomycin is absent from Escherichia coli and other gram-negative pathogens, Antimicrobial agents and chemotherapy, 57 (2013) 637-639.

[29] A.R.Stokes and A.J.C.Wilson, The diffraction of X-rays by distorted crystal aggregates-I, Proceedings of the Physical Society, 56 (1944) 174-181.

[30] R. Bos, H.C. van der Mei and H.J. Busscher, Physico-chemistry of initial microbial adhesive interactions - its mechanisms and methods for study, Fems Microbiology Reviews, 23 (1999) 179-230.

[31] T. Hamouda and J.R. Baker, Antimicrobial mechanism of action of surfactant lipid preparations in enteric Gram-negative bacilli, Journal of Applied Microbiology, 89 (2000) 397-403.

[32] S. Tougaard, Accuracy of the non-destructive surface nanostructure quantification technique based on analysis of the XPS or AES peak shape, Surface and Interface Analysis, 26 (1998) 249-269.

[33] Y.H. Leung, C.M. Chan, A.M. Ng, H.T. Chan, M.W. Chiang, A.B. Djurisic, Y.H. Ng, W.Y. Jim, M.Y. Guo, F.C. Leung, W.K. Chan and D.T. Au, Antibacterial activity of ZnO nanoparticles with a modified surface under ambient illumination, Nanotechnology, 23 (2012) 475703.

[34] T. Hirakawa, K. Yawata and Y. Nosaka, Photocatalytic reactivity for O_2^- and OH radical formation in anatase and rutile TiO_2 suspension as the effect of H_2O_2 addition, Applied Catalysis A: General, 325 (2007) 105-111.

[35] T. Hirakawa and Y. Nosaka, Properties of O_2^-• and OH• Formed in TiO_2 Aqueous Suspensions by Photocatalytic Reaction and the Influence of H_2O_2 and Some Ions, Langmuir, 18 (2002) 3247-3254.

[36] M.C. Lee, F. Yoshino, H. Shoji, S. Takahashi, K. Todoki, S. Shimada and K. Kuse-Barouch, Characterization by electron spin resonance spectroscopy of reactive oxygen species generated by titanium dioxide and hydrogen peroxide, Journal of Dental Research, 84 (2005) 178-182.

[37] B.J. Juven and M.D. Pierson, Antibacterial effects of hydrogen peroxide and methods for its detection and quantitation, Journal of Food Protection, 59 (1996) 1233-1241.

[38] R.A. Palominos, M.A. Mondaca, A. Giraldo, G. Penuela, M. Perez-Moya and H.D. Mansilla, Photocatalytic oxidation of the antibiotic tetracycline on TiO_2 and ZnO suspensions, Catalysis Today, 144 (2009) 100-105.

[39] Y. Kikuchi, K. Sunada, T. Iyoda, K. Hashimoto and A. Fujishima, Photocatalytic bactericidal effect of TiO2 thin films: Dynamic view of the active oxygen species responsible for the effect, Journal of Photochemistry and Photobiology a-Chemistry, 106 (1997) 51-56.

[40] N. Padmavathy and R. Vijayaraghavan, Enhanced bioactivity of ZnO nanoparticles—an antimicrobial study, Science and Technology of Advanced Materials, 9 (2008) 035004.

[41] F.Q. Tang, Y. Sakka and T. Uchikoshi, Electrophoretic deposition of aqueous nano-sized zinc oxide suspensions on a zinc electrode, Materials Research Bulletin, 38 (2003) 207-212.

[42] C. Maneerat and Y. Hayata, Antifungal activity of TiO2 photocatalysis against Penicillium expansum in vitro and in fruit tests, International Journal of Food Microbiology, 107 (2006) 99-103.

[43] B. Halliwell and J.M. Gutteridge, Oxygen toxicity, oxygen radicals, transition metals and disease, Biochemical Journal, 219 (1984) 1-14.

[44] R.A. Palominos, M. A. Mondaca, A. Giraldo, G. Penuela, M. Perez-moya & H. D. Mansilla, Photocatalytic oxidation of the antibiotic tetracycline on TiO2 and ZnO suspensions. Catalysis Today, 144 (2009) 100-105.

Research Highlights

- ZnO NPs without contacting with bacterial cells showed strong antibacterial effect.
- ZnO NPs caused cell death by directly interacted with the phospholipid bilayer of the membrane due to the electrostatic attraction and causing loss of membrane integrity.
- Traces of zinc ions and hydrogen peroxide were detected in ZnO NPs suspensions, but was insufficient to cause the antibacterial effect.
- The addition of radical scavengers results showed the generation of ROS, especially hydroxyl radicals, played an important role in the antibacterial properties of ZnO NPs.